Supplementary Information (SI) for New Journal of Chemistry.
This journal is © The Royal Society of Chemistry and the Centre National de la Recherche Scientifique 2026

Supplementary Information

Redox-active chromophore grafted microenvironment in metal-organic framework recognizes aromatic amine isomers

Bijan Sarkar[a], Suvendu Panda,[a‡] KM Archana Yadav,[a‡] Chaitanya Yerragudi,[b‡] Niharika Mahala,[a‡] Rajarshi Ghosh,[a] Pralok K. Samanta,[c] Nivedita Sikdar,[b] Ritesh Haldar*[a]

a. Tata Institute of Fundamental Research Hyderabad, Gopanpally, Hyderabad 500046, Telangana, India.

b. Department of Chemistry, GITAM School of Science Hyderabad, Telangana 502329, India.

c. Department of Chemistry, Birla Institute of Technology and Science (BITS) Pilani, Hyderabad Campus, Hyderabad 500078, India.

1. Characterization techniques

1.1. Powder X-ray diffraction (PXRD)

Powder X-ray diffractometer (XRD) patterns of MOF-powders were recorded on a Rigaku XDS 2000 diffractometer using nickel-filtered Cu *K*α radiation (λ = 1.5418 Å) ranging from 5° to 30 ° at room temperature (voltage 40 kV, current 200 mA) with a scan rate 0.7 º/s.

1.2. Scanning electron microscopy (SEM)

The surface morphology of the MOF-808 powders were characterized using field emission scanning electron microscopy (FESEM), JEOL JSM-7200F instrument with a cold emission gun operating at 30 kV.

1.3. Infrared spectroscopy

Attenuated total reflection (ATR) absorption spectroscopy of the MOF powders was done using the Bruker Vertex 70v instrument, with a spectral resolution of 2 cm^{-1}.

1.4. X-ray photoelectron spectroscopy

Elemental detection of the powders were performed using X-ray photoelectron spectrometer (PHI versaProbe III) within an ultrahigh vacuum (1×10^{-9} bar) environment. This instrument was equipped with an Al-*K*α X-ray source and a monochromator

1.5. UV-Visible diffuse reflectance spectroscopy

Diffuse reflectance UV-visible spectroscopy was carried out using a Shimadzu 2600 spectrophotometer

1.6. Nuclear magnetic resonance (NMR) spectroscopy

NMR spectra were recorded on a Bruker NanoBay 300 MHz NMR spectrometer. Incorporation and integration of NMI at MOF-808 powders was checked through NMR data. 10 mg of MOF powder was digested in a HF/DMSO-d_6 (50µL/0.4ml) solution. The entire solution was submitted for NMR.

1.7. EPR measurements

Electron paramagnetic resonance (EPR) measurements were performed using the magnettech ESR5000 spectrometer operating in the X-band frequency range (~9.4 GHz) with a continuous-wave (CW) detection mode at 25°C.

1.8. Fluorescence

Steady-state fluorescence was recorded by the Fluorolog-QM™ (Horiba Scientific). For the time-resolved spectroscopy, DeltaFlex™ (Horiba Scientific) was used.

2. Experimental section

2.1. Chemicals

Zirconyl chloride octahydrate $ZrOCl_2 \cdot 8H_2O$ (Sigma Aldrich), 1,3,5-benzenetricarboxylic acid (TCI), acetic acid (SRL), 4-aminobenzoic acid (TCI), N, N-Dimethylformamide (DMF) (Merck), Sodium acetate trihydrate (TCI), Ethanol (RCP), 1,2-phenylenediamine (TCI), 1,3-phenylenediamine (TCI), 1,4-phenylenediamine (Sigma), Potassium Dichromate (SRL), Chromium Trioxide (SRL). All the above chemicals have been used without further purification.

2.2. Synthesis of MOF-808, $Zr_6(\mu_3\text{-}O)_4(\mu_3\text{-}OH)_4(CH_3COO)_{4.28}(BTC)_2(OH)_{1.72}$

MOF-808 was synthesised using a slightly modified reported procedure.[1] A mixture of 1,3,5-benzenetricarboxylic acid (280 mg, 1.33 mmol), $ZrOCl_2 \cdot 8H_2O$ (1.288 g, 4 mmol), water (10 mL), and acetic acid (10 mL) was heated at 100 °C for 24 hours. After the reaction, the resulting suspension was centrifuged**.** The precipitate was then washed twice by re-dispersing in 15 mL

of 0.1 M aqueous sodium acetate solution, followed by washing with water. The Resulting white colour powder was then evacuated at 150 °C for 24h.

2.3. Synthesis of ZrOH-BTC, $Zr_6(\mu_3\text{-}O)_4(\mu_3\text{-}OH)_4(CH_3COO)_{0.1}(BTC)_2(OH)_{5.9}$

250 mg of activated MOF-808 was dispersed in a 55 ml DMF solution, 5 ml of HCL 1(M) was added. The mixture was heated at 80 °C for 24 hours. After the reaction the suspension was centrifuged, and the precipitate was washed by DMF. The Resulting white colour powder was then evacuated at 150 °C for 24h.

2.3 Synthesis of Naphthaleneimide (NMI)

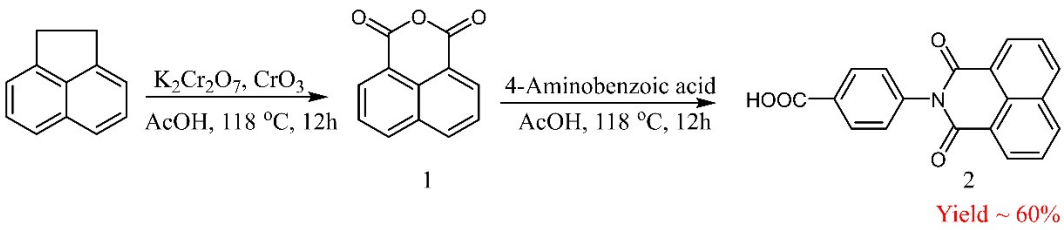

Scheme S1. Synthesis scheme of 4-(1,3-dioxo-1H-benzo[de]isoquinolin-2(3H)-yl)benzoic acid

1H,3H-benzo[de]isochromene-1,3-dione (1) was synthesized by a previously reported method.[2] Acenaphthene (1 g, 6.48 mmol), K2Cr2O7 (6.79 g, 25.94 mmol) and CrO3 (1.29 g, 12.96mmol) were mixed in 30 ml glacial acetic acid and heated to 120 °C For 12h. The reaction mixture was cooled and poured into water; the greenish precipitate was washed with 1 M HCL and DI water. We performed the next step with purifying the product.

4-(1,3-dioxo-1H-benzo[de]isoquinolin-2(3H)-yl)benzoic acid (2) was synthesized following an earlier reported method.[3] 1,8-naphthalic anhydride (1.98 g, 10 mmol), 4-aminobenzoic acid (1.37 g, 10 mmol), and AcONa (2.48 g, 30 mmol) were mixed in 30 ml glacial acetic acid. The reaction mixture was heated to 120 °C for overnight under N_2 atmosphere. After 12h, the mixture was cooled to room temperature and poured into water. A yellow precipitate was collected and washed several times with acetic acid and water. UV (λ_{max}, nm): 334 (40 µM in DMF). IR (ATR, 1697 cm^{-1}, 1660 cm^{-1}, 1587 cm^{-1}, 1238 cm^{-1}) ^{1}H-NMR (300 MHz; DMSO-d_6): δ 8.5456-8.5138 (m, 4H), 8.1096-8.0832 (d, 2H, J = 3.27 Hz), 7.9473-7.8595 (t, 2H, J = 7.92 Hz), 7.5641-7.5426 (d, 2H, J = 7.94 Hz).

2.4. Synthesis of MOF-808- NMI

NMI incorporation was done by the following procedure.[4] Naphthaleneimide (NMI) (200 mg, 0.63 mmol) was dissolved in 5 ml of DMF. Then MOF-808 (200 mg, 0.138 mmol) was added to the solution and was heated at 100 °C for 24 hours. The reaction mixture cooled to room temperature, the suspension was centrifuged and washed with DMF and water. The white solid was vacuum-dried. The excess naphthaleneimide that was not co-ordinatively bonded with Zr was removed by refluxing in ethanol for 24 hours.

2.5. Confinement of phenylenediamine isomers in MOF-808-NMI

0.14 M ethanol solutions of three phenylenediamine isomers-1,2-phenylenediamine (ortho), 1,3-phenylenediamine (meta), and 1,4-phenylenediamine (para)-were prepared. Each amine solution was added individually to separate vials containing 20mg of activated MOF-808-NMI. The resulting suspensions were stirred at room temperature for 24 h to allow incorporation of the amines into the MOF framework. During this period, distinct color changes were observed for each isomer, indicating successful interaction with the confined environment of the MOF. After completion of the loading process, the suspensions were centrifuged to collect the solids. The recovered samples were sonicated and washed thoroughly with ethanol several times to remove any unbound amine molecules. Finally, the obtained powders were dried under vacuum, and the resulting materials were used for further characterization.

2.6. Electrochemical Characterization:

All measurements were carried out in 0.1 M tetrabutylammonium perchlorate (TBAP) in acetonitrile. For NMI measurements, 5 mg of naphthaleneimide was dispersed in 35 mL electrolyte (corresponding to ~0.5 mM NMI). The MOF-808-NMI working electrode was prepared by dispersing 1 mg of the composite in 200 µL of catalyst ink (water: IPA: Nafion = 4.9: 4.9: 0.2 mL), and 6 µL of this ink was drop-cast onto a 3 mm glassy carbon electrode to give a loading of ~0.42 mg cm^{-2}. For amine-interaction studies, 2 mg of each phenylenediamine isomer (o-, m-, p-PDA) was dissolved in 35 mL of electrolyte, giving a final concentration of 0.53 mM for each amine solution. Cyclic voltammetry was performed at a scan rate of 50 mV s^{-1} *vs* with an Ag/AgCl reference electrode.

2.7. Calculation details

Geometry optimisations of all the compounds are carried out with the aid of density functional theory (DFT) using B3LYP exchange-correlation functional and 6-31G(d) basis set as implemented in Gaussian 09 suite of programs.[5]

3. Table-1

Sample	$\tau_1\ (ns)$	$\tau_2\ (ns)$	$\tau_3\ (ns)$
MOF-808-NMI	0.2	0.2	3.3
m-PDA@MOF-808-NMI	0.13	1.51	0.13

4. Figures

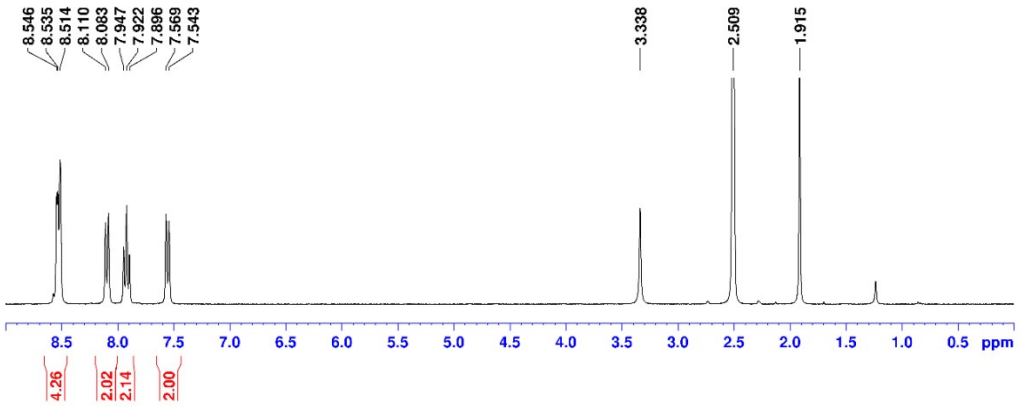

Fig. S1. ^{1}H-NMR data of 4-(1,3-dioxo-1H-benzo[de]isoquinolin-2(3H)-yl) benzoic acid

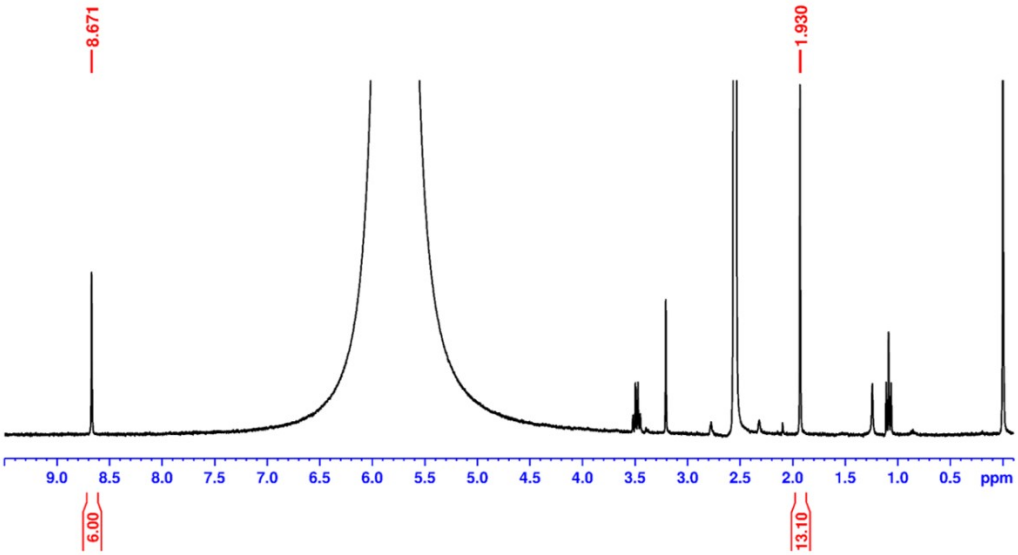

Fig. S2. ^{1}H-NMR data of the digested MOF-808, $Zr_6(\mu_3\text{-}O)_4(\mu_3\text{-}OH)_4(CH_3COO)_{4.28}(BTC)_2(OH)_{1.72}$

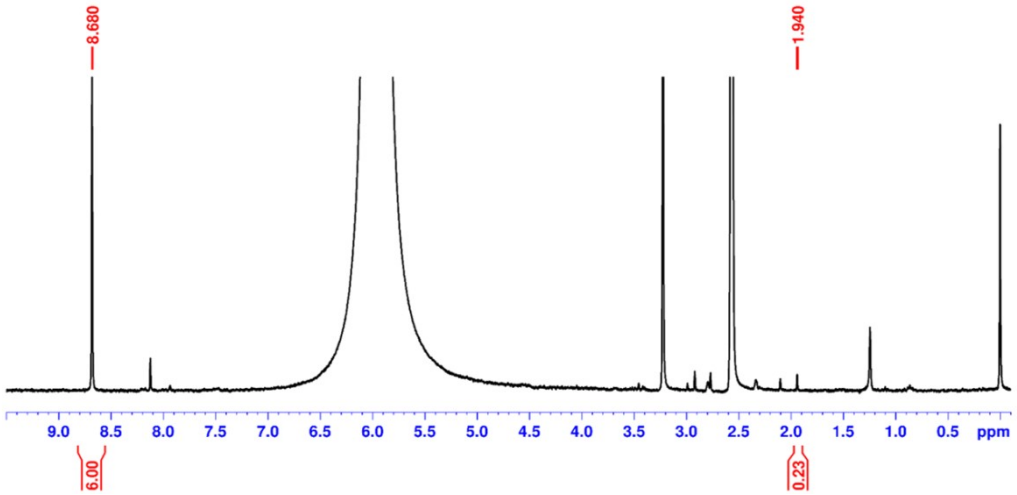

Fig. S3. ^{1}H-NMR data of the digested ZrOH-BTC, $Zr_6(\mu_3\text{-}O)_4(\mu_3\text{-}OH)_4(CH_3COO)_{0.1}(BTC)_2(OH)_{5.9}$

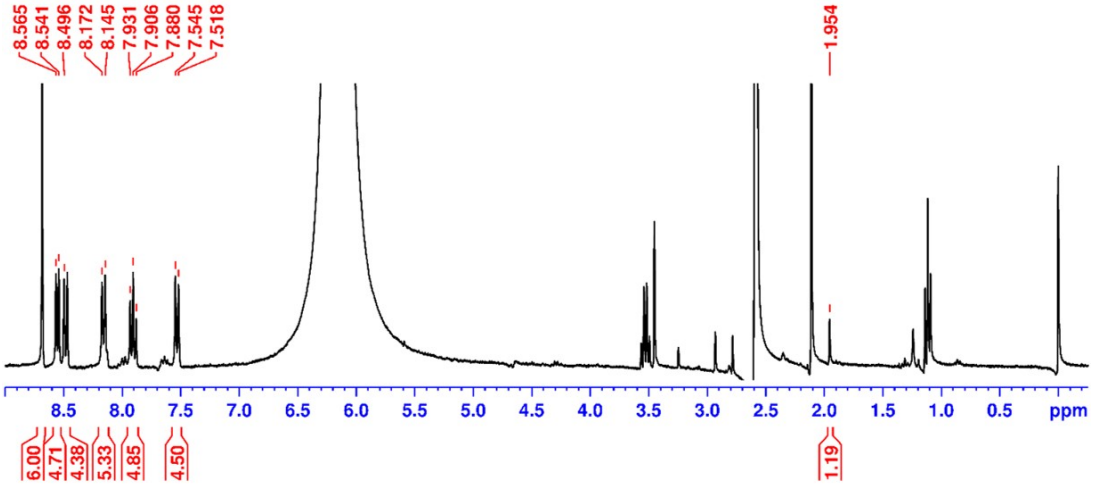

Fig. S4. ^{1}H-NMR data of the digested MOF-808-NMI, $Zr_6(\mu_3\text{-}O)_4(\mu_3\text{-}OH)_4(CH_3COO)_{0.4}(NMI)_{2.3}(BTC)_2(OH)_{3.3}$

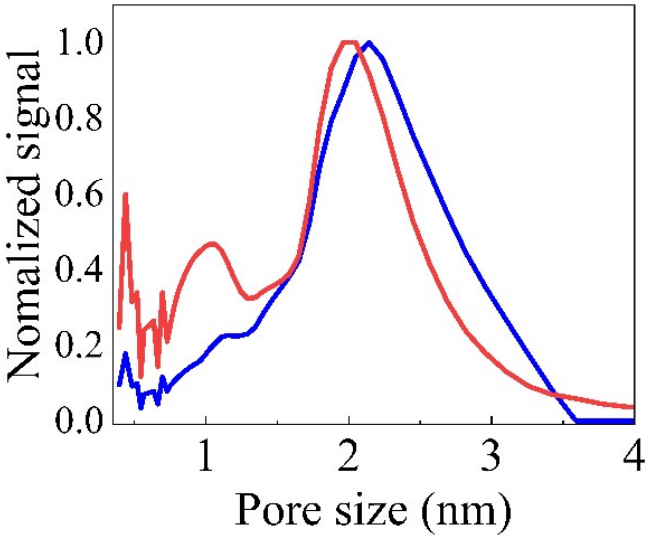

Fig. S5. Pore size distribution of MOF-808(Blue) and MOF-808-NI (Red).

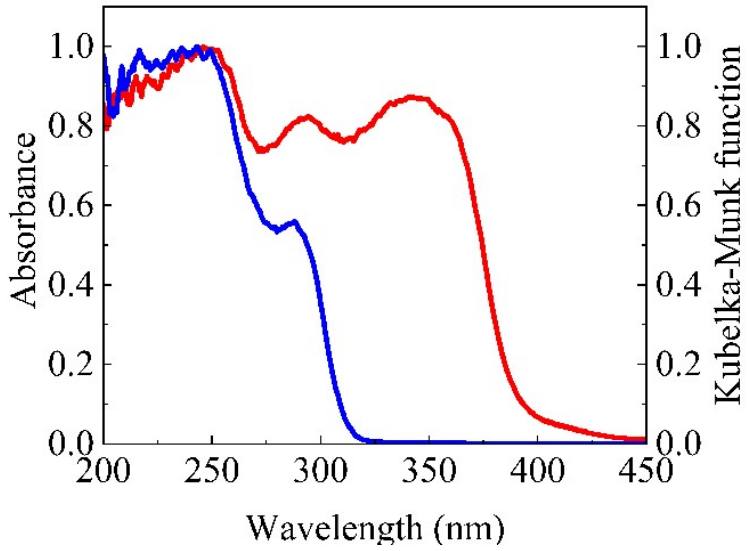

Fig. S6. UV-DRS data of MOF-808(Blue) and MOF-808-NI (Red).

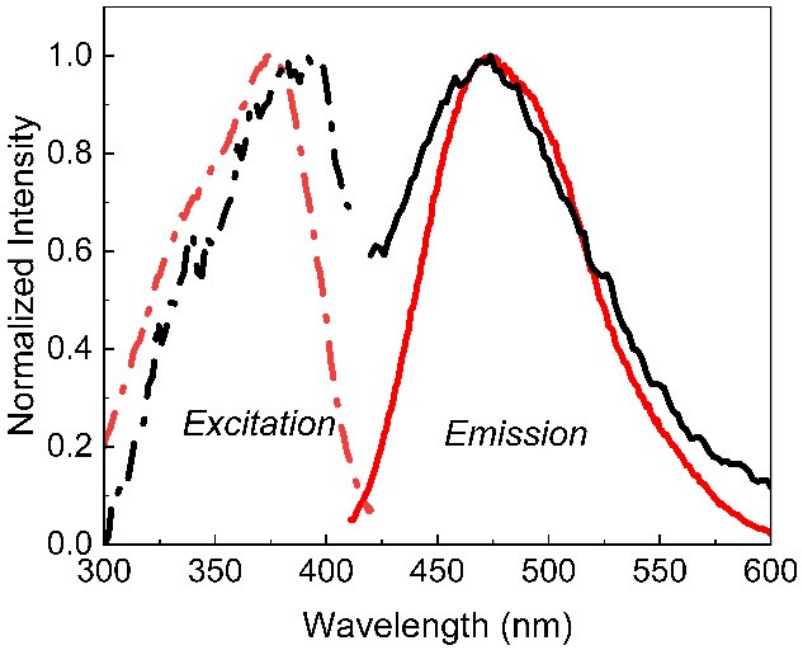

Fig. S7. Black: Emission (monitored at 330nm) and excitation (monitored at 475nm) spectra of solid NMI powder, Red: Emission (monitored at 330nm) and excitation (monitored at 475nm) spectra of MOF-808-NI.

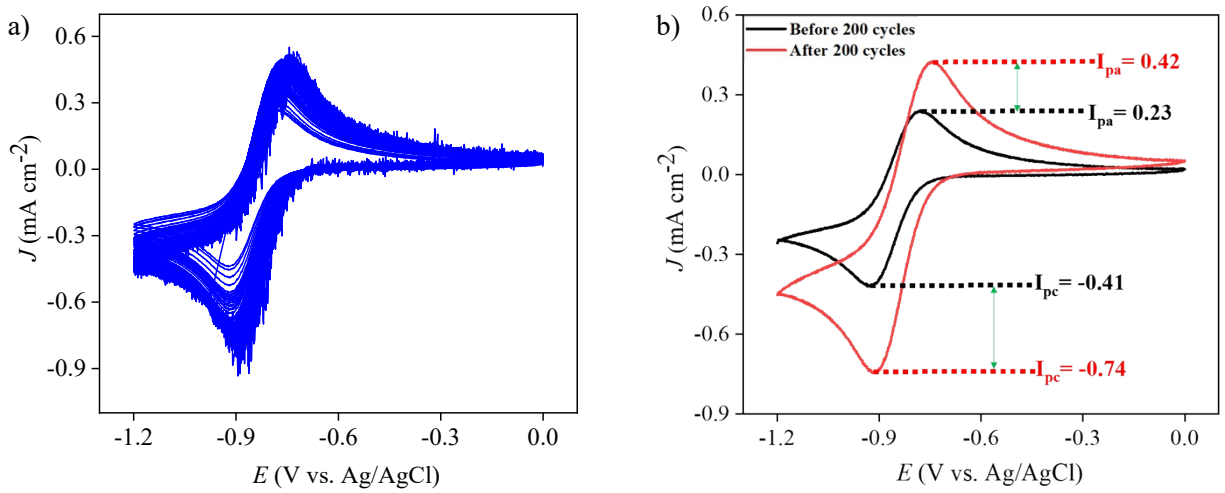

Fig. S8. a) Cyclic voltammogram of MOF-808-NMI for 200 continuous cycles, b) Comparison of anodic and cathodic peak current densities before and after 200 cycles.

We carried out 200 continuous cyclic voltammetry (CV) cycles under the same electrochemical conditions described in the manuscript (Figure 3b). The redox peaks associated with the NMI remain clearly visible even after 200 cycles, indicating that the NMI units are electrochemically stable in the MOF-808. If the chromophore had detached or degraded during repeated measurements, a noticeable decrease or disappearance of the peaks would be expected;

however, this was not observed. Instead, the anodic peak current increases from 0.23 to 0.42 mA cm^{-2} (an 82.6% increase), and the cathodic peak current increases from −0.41 to −0.74 mA cm^{-2} (an 80.5% increase). The enhancement of both oxidation and reduction currents suggest gradual electrolyte penetration into the porous structure and improved accessibility of redox-active sites upon cycling.

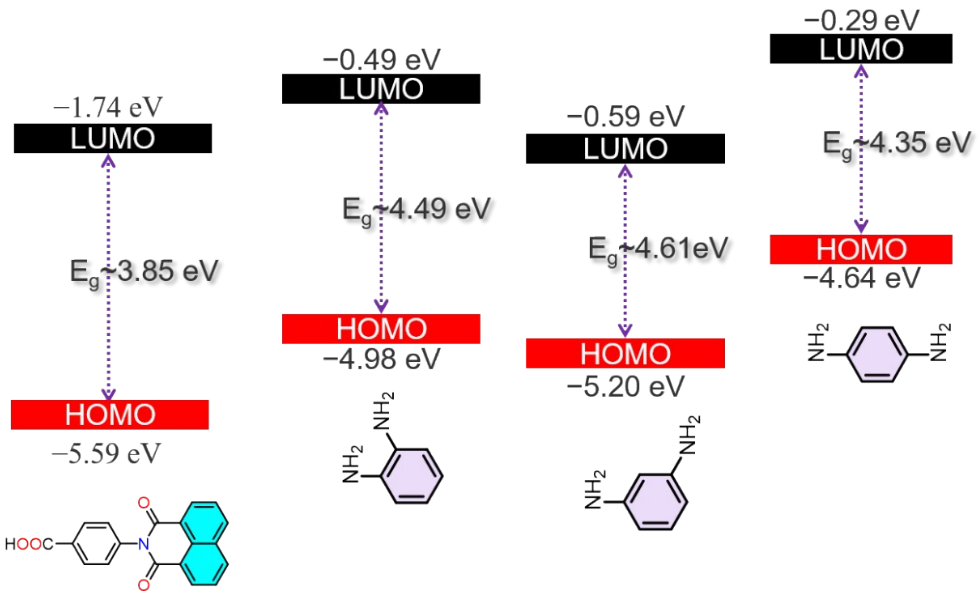

Fig. S9. Calculated energy level diagram of NMI, o-PDA, m-PDA, and p-PDA.

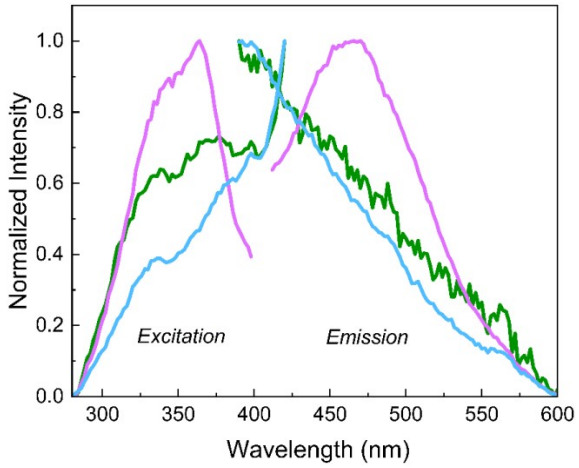

Fig. S10. Green: Emission (monitored at 330nm) and excitation (monitored at 475nm) spectra monitored for *o*-PDA@MOF-808-NMI (green), *m*-PDA@MOF-808-NMI (purple), and *p*-PDA@MOF-808-NMI (blue).

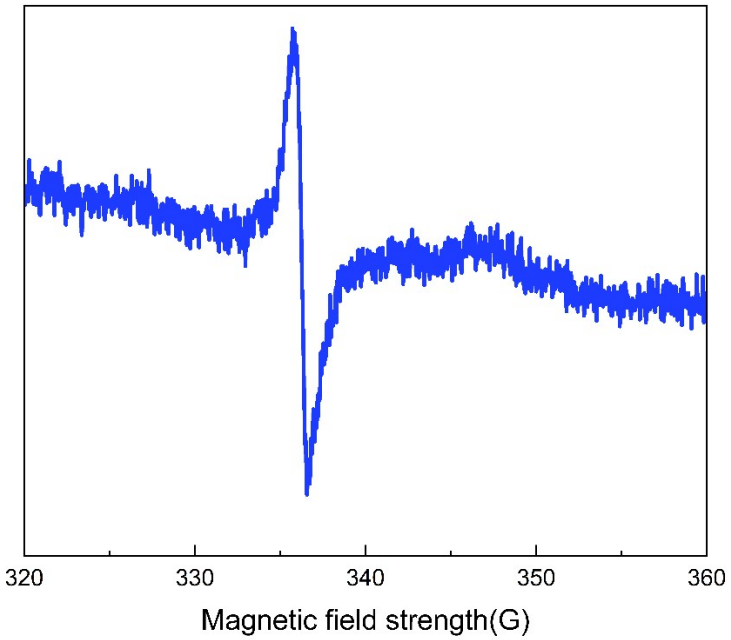

Fig. S11. EPR signal for *p*-PDA@MOF-808-NMI, synthesized at dark condition and low temperature (4 °C).

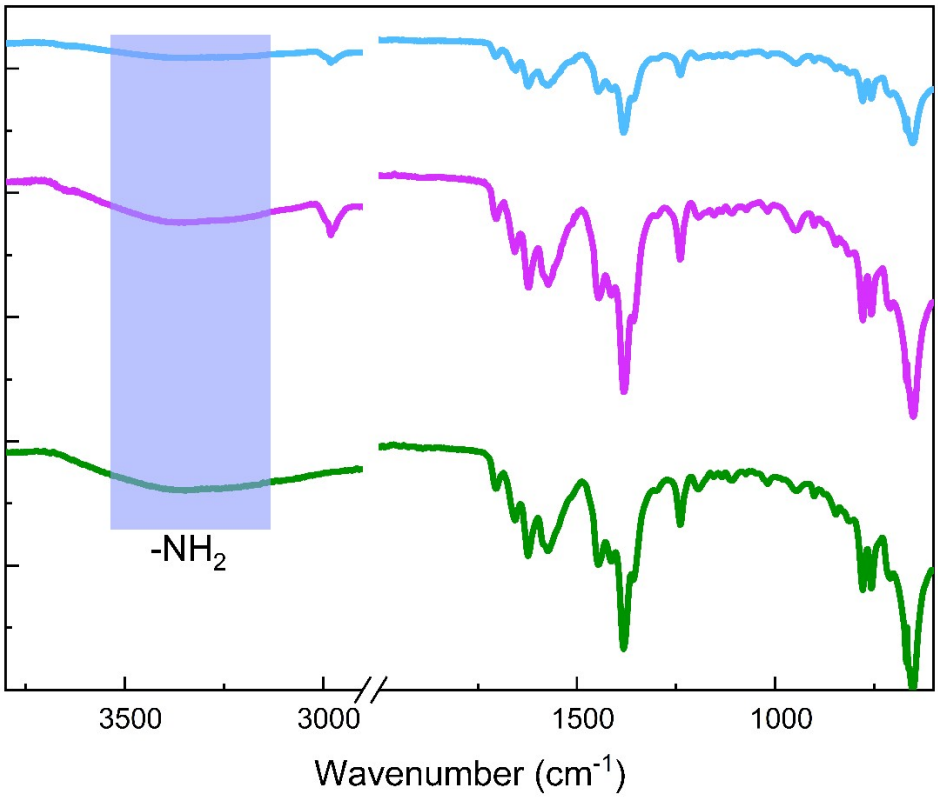

Fig. S12. ATR-IR data of o-PDA@MOF-808-NMI (green), m-PDA@MOF-808-NMI (purple), and p-PDA@MOF-808-NMI (blue).

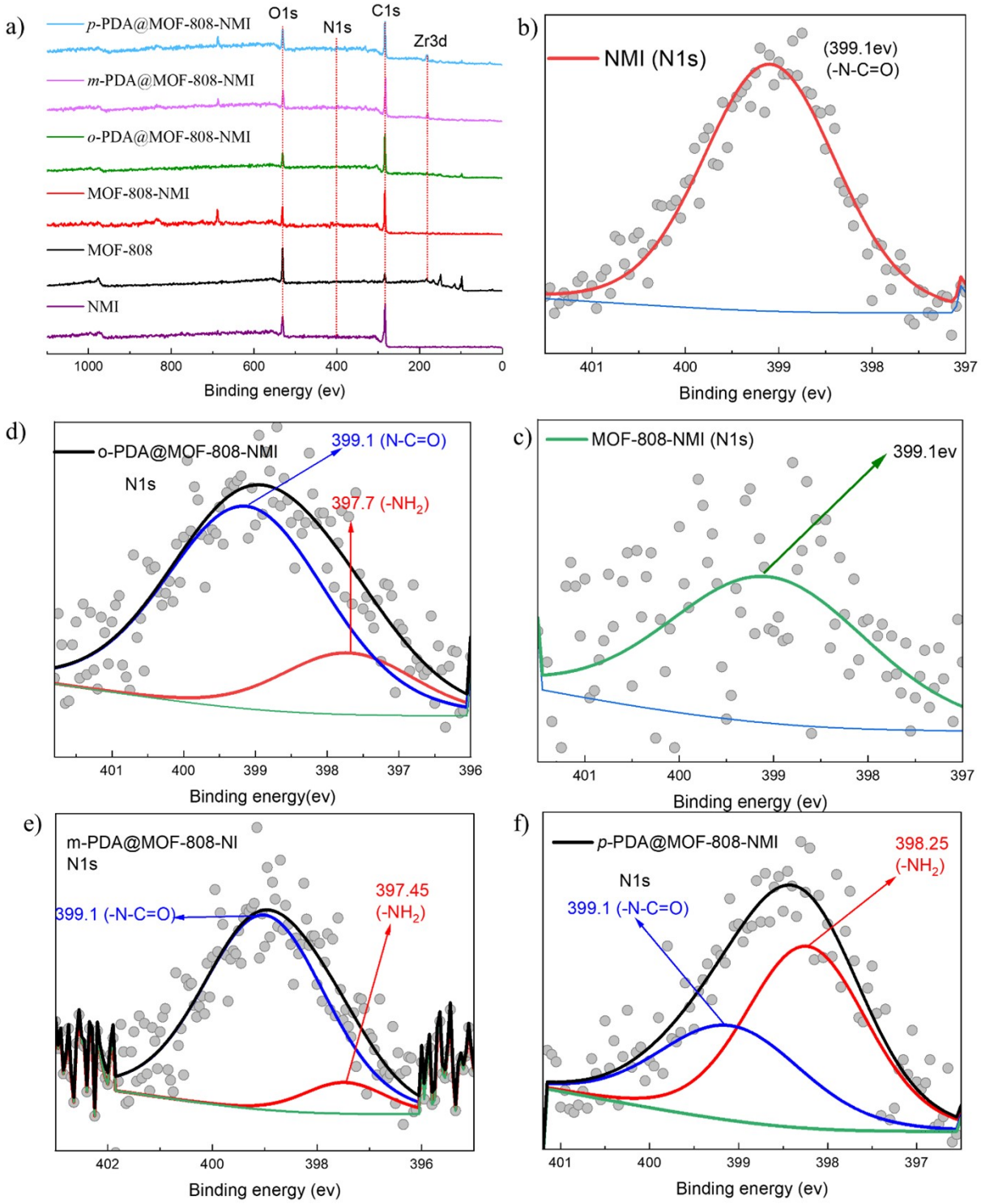

Fig. S13. XPS comparison of NMI, MOF-808, MOF-808-NMI, *o*-PDA@MOF-808-NMI, *m*-PDA@MOF-808-NMI, and *p*-PDA@MOF-808-NMI. a) Overview scan; b),c),d),e), and f) high resolution scan of N1S.

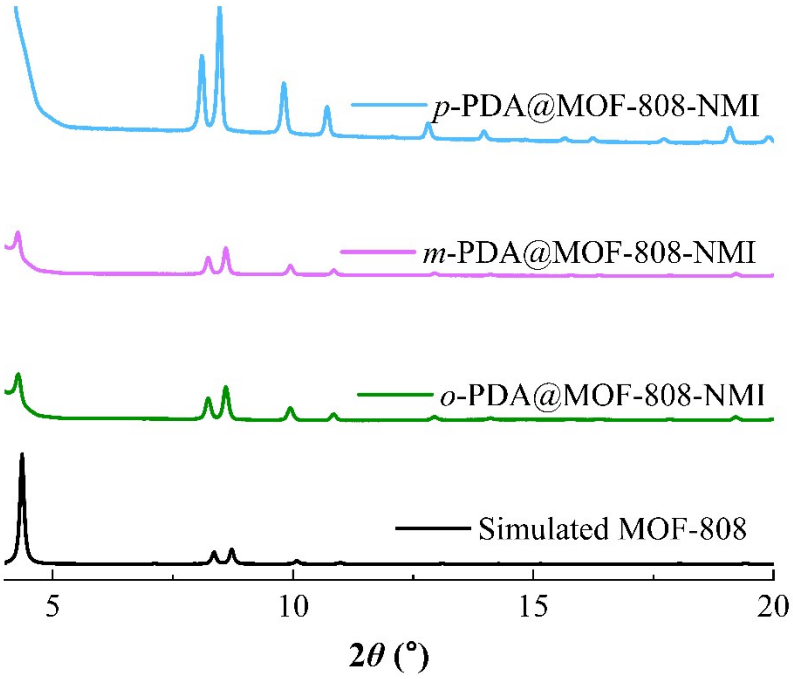

Fig. S14. PXRD data of o-PDA@MOF-808-NMI (green), m-PDA@MOF-808-NMI (purple), and p-PDA@MOF-808-NMI (blue).

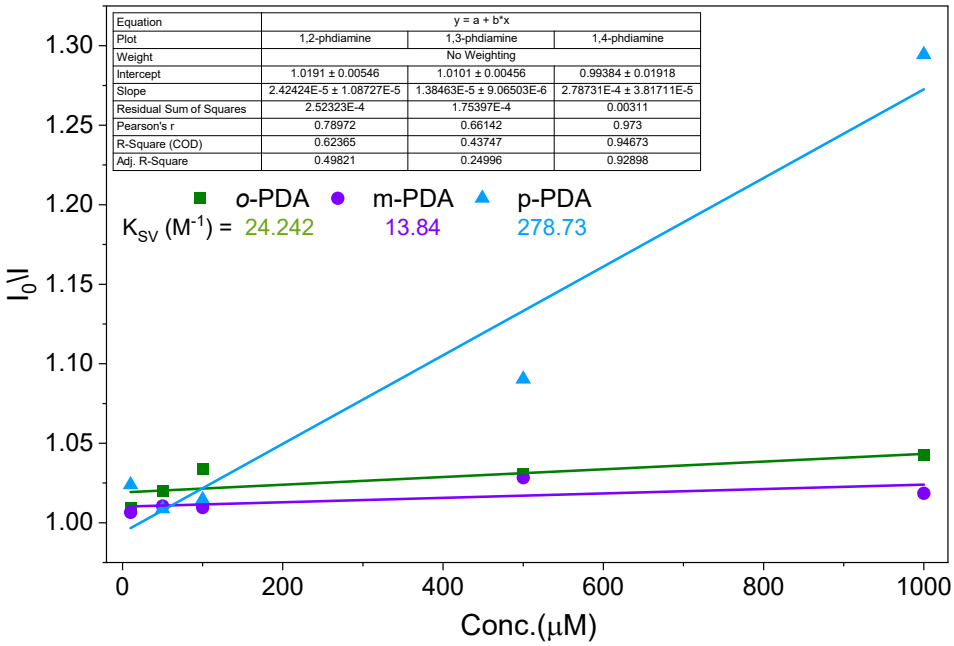

Fig. S15. Stern-Volmer plots for the different PDA fluorescence sensing. K_{SV} is the quenching constant.

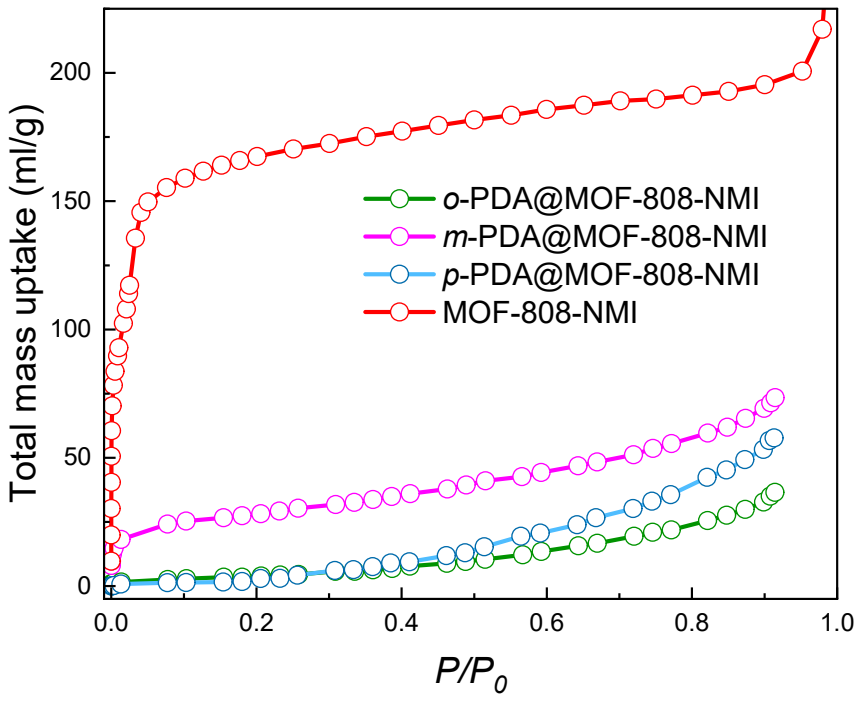

Fig. S16. N_2 adsorption isotherms at 77 K, P_0 is 760 mmHg.

1. H. Reinsch, S. Waitschat, S. M. Chavan, K. P. Lillerud and N. Stock, *European Journal of Inorganic Chemistry*, 2016, **2016**, 4490-4498.
2. M. Verma, V. Luxami and K. Paul, *RSC Advances*, 2015, **5**, 41803-41813.
3. A. M. M. El-Betany and N. B. McKeown, *Tetrahedron Letters*, 2012, **53**, 808-810.
4. M. Sharifi-Rad, M. Kaykhaii, M. Khajeh and A. Oveisi, *BMC Chemistry*, 2022, **16**, 27.
5. Gaussian 09, Revision A.02, M. J. Frisch, G. W. Trucks, H. B. Schlegel, G. E. Scuseria, M. A. Robb, J. R. Cheeseman, G. Scalmani, V. Barone, G. A. Petersson, H. Nakatsuji, X. Li, M. Caricato, A. Marenich, J. Bloino, B. G. Janesko, R. Gomperts, B. Mennucci, H. P. Hratchian, J. V. Ortiz, A. F. Izmaylov, J. L. Sonnenberg, D. Williams-Young, F. Ding, F. Lipparini, F. Egidi, J. Goings, B. Peng, A. Petrone, T. Henderson, D. Ranasinghe, V. G. Zakrzewski, J. Gao, N. Rega, G. Zheng, W. Liang, M. Hada, M. Ehara, K. Toyota, R. Fukuda, J. Hasegawa, M. Ishida, T. Nakajima, Y. Honda, O. Kitao, H. Nakai, T. Vreven, K. Throssell, J. A. Montgomery, Jr., J. E. Peralta, F. Ogliaro, M. Bearpark, J. J. Heyd, E. Brothers, K. N. Kudin, V. N. Staroverov, T. Keith, R. Kobayashi, J. Normand, K. Raghavachari, A. Rendell, J. C. Burant, S. S. Iyengar, J. Tomasi, M. Cossi, J. M. Millam, M. Klene, C. Adamo, R. Cammi, J. W. Ochterski, R. L. Martin, K. Morokuma, O. Farkas, J. B. Foresman, and D. J. Fox, Gaussian, Inc., Wallingford CT, 2016.